AIP | Review of Scientific Instruments

High temperature Z-meter setup for characterizing thermoelectric material under large temperature gradient

R. Amatya, P. M. Mayer, and R. J. Ram

Citation: Review of Scientific Instruments **83**, 075117 (2012); doi: 10.1063/1.4731650
View online: http://dx.doi.org/10.1063/1.4731650
View Table of Contents: http://scitation.aip.org/content/aip/journal/rsi/83/7?ver=pdfcov
Published by the AIP Publishing

High temperature Z-meter setup for characterizing thermoelectric material under large temperature gradient

R. Amatya,[a] P. M. Mayer,[b] and R. J. Ram
Research Laboratory of Electronics, Massachusetts Institute of Technology, 77 Massachusetts Ave, Cambridge, Massachusetts 02139, USA

(Received 26 January 2012; accepted 4 June 2012; published online 30 July 2012)

To properly estimate a thermoelectric material's performance, one should be able to characterize a single thermoelectric (TE) element with a large temperature gradient. In this work, we present an experimental setup including a Z-meter that can heat the sample to a very high temperature of 1200 °C in vacuum. The Z-meter can simultaneously measure all three thermoelectric parameters (Seebeck coefficient, thermal conductivity, and electrical conductivity), as well as measure the generated power and the efficiency for a single TE leg. Furthermore, this measurement of power conversion efficiency is used to generate a measure of the material's *ZT*. An *in situ* metallurgical bond was used to achieve low thermal (0.05 Kcm^2/W) and electrical (3 mΩ) contact parasitics. An integrated strain gauge ensures reproducible thermal contact. At high temperature (>600 K), radiative heat transfer is modeled and the instrument is optimized to suppress the systematic error to below 7%. The TE parameters and *ZT* for a bulk-sample (Bi_2Te_3) and a thin-film sample (ErAs:InGaAlAs) with a large temperature gradient ($\Delta T \sim 200$ K) have been measured and are within 3%–7% of the independently measured values. © *2012 American Institute of Physics*. [http://dx.doi.org/10.1063/1.4731650]

I. INTRODUCTION

With the benefits of no noise, no moving parts, and low maintenance, a thermoelectric (TE) generator, based on the Seebeck effect, can be an attractive alternative power source for today's energy demands. A good TE material characterized by a dimensionless figure-of-merit ($ZT = ((\alpha^2\sigma)/\kappa)$ T) has low thermal conductivity (κ), high electrical conductivity (σ), and high Seebeck coefficient (α).[1] Here, T is the absolute temperature of the thermoelectric material at its operating point. A simple TE generator consists of p- and n-type semiconductor legs connected electrically in series and thermally in parallel (Fig. 1). For a generator, not only high *ZT* is important, but a large temperature gradient across the generator also increases the maximum achievable thermal-to-electrical conversion efficiency (η_{max}) given by[1]

$$\eta_{max} = \frac{T_h - T_c}{T_h} \cdot \frac{\sqrt{1 + ZT_M} - 1}{\sqrt{1 + ZT_M} + T_c/T_h}. \quad (1)$$

Here, T_h is the hot side temperature, T_c is the cold side temperature, and T_M is the average temperature of the TE material.

The TE parameters (σ, α and κ) are temperature dependent and are typically measured independently with a small temperature gradient ($\Delta T \sim 1$ or 2 K) around the mean operating temperature (T).[2] However, to properly estimate a thermoelectric generator's performance under large temperature differentials, across which the thermoelectric parameters may vary significantly, it is desirable to characterize the elements with a large temperature gradient. Conventionally, the TE parameters are measured using different measurement tools and different contacts and sample geometries. *ZT* values obtained from assembling such measurements can have high uncertainty, not only due to measurement errors but also due to sample variability.[3] For example, the van der Pauw's method is a common technique to measure the electrical conductivity of an arbitrarily shaped sample.[4,5] This four-point probe technique requires the current flow be approximately two-dimensional for accurate results.[4] The standard way of measuring the Seebeck coefficient is by applying a small temperature gradient across a TE sample and varying the average temperature.[3] At each temperature, the ratio of the open circuit voltage to the temperature gradient gives the Seebeck coefficient. Thermal diffusivity measurements are widely used to measure material's thermal conductivity.[3,6] Accurate specific heat data are required simultaneously with the thermal diffusivity value to obtain thermal conductivity from this method.[3] Apart from individual parameter measurement synthesized to evaluate *ZT*, another method to extract *ZT* directly is the transient Harman technique.[7,8] Adiabatic boundary conditions are required for this method, and only a small temperature difference across the sample can be applied during the measurement.[7,9] Many variants of this technique have been used to measure properties of TE samples.[10,11]

Another experimental system for *ZT* measurement is the Z-meter. It is an instrument that measures the three TE parameters of interest (σ, α, and κ) as a function of temperature from which *ZT* can be calculated. The advantage of Z-meter measurement over other techniques is that all three TE parameters are measured from a single sample simultaneously. Apart from measuring individual TE parameters, the tool can be used to measure generator performance parameters such as thermal-to-electrical conversion efficiency and power density for the TE sample. Some of the key aspects and limitations of previous work on the Z-meter are summarized in Table I.

[a]Tel: (617)-253-2125. email: ramatya@mit.edu.
[b]Currently at Physical Sciences Inc., MA.

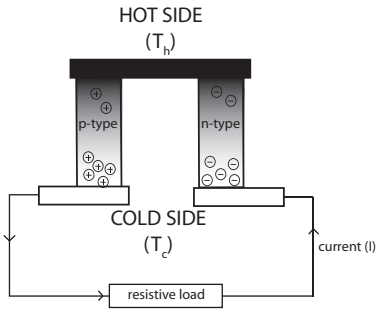

FIG. 1. A simple TE generator with a p- and n-type leg connected electrically in series with a resistive load.

The systems described in previous work have mostly been for thick sample (thickness > 1 mm) characterization. When it comes to short-leg and thin-film samples (<500 μm), there are no Z-meter setups that can give accurate results with high temperature (>500 K) measurement capabilities. We have adopted a variant of the Z-meter setup described in Ref. 12 and improved on its parasitic performance as well as worked on making it a flexible system for various temperature ranges. Here, we present a Z-meter system which is used to characterize thin-film TE samples (thickness $\sim$ 100s μm) as well as thick bulk materials. When measuring thin-film samples, the system parasitics become very important; they have been addressed in this setup to minimize errors. Even for a thick TE sample (thickness $\sim$ 1.5 mm) used in commercial modules (Bi_2Te_3 based), the internal resistance for a single leg with a typical aspect ratio can be as low as 10–15 mΩ. Any Z-meter for individual TE elements has to accurately measure such small resistances. Both intrinsic thermal and electrical resistances for TE samples decrease with thickness, and the system parasitics become dominant in such measurements.

The Z-meter described in Ref. 13 can measure the TE properties in the range of 100–600 °C, but each parameter is measured under different temperature gradients. Some Z-meters are limited by the system parasitic resistance (30 mΩ) which is inadequate for precise electrical conductivity measurements for a single leg.[14] High temperature (100–1300 K) electrical resistivity and Seebeck coefficient measurement setup is described in Ref. 15, where the maximum temperature gradient is limited to 20 K. A commercial Z-meter from RMT Ltd. is used to characterize TE modules and is not meant for single TE element characterization.[16] The experimental setup described in Ref. 17 shows measurement under large temperature gradient (160 °C) for hot side temperature of 200 °C. In this referenced work, rather than characterizing the system parasitics to get actual material TE parameters, effective *ZT* values were measured with lumped parasitics.

In this work, we present an experimental dc measurement technique with a Z-meter to measure the TE properties of a material under practical working conditions of a generator, i.e., with a large temperature gradient ($\sim$200 K), for a wide range of average sample temperatures. Simultaneous measurements are used to extract all three TE properties to determine the *ZT* values. Also, the tool allows for a direct measurement of the conversion efficiency which can be used to extract *ZT*. Apart from *ZT*, the measurement also gives the power density for a single TE element, which can be crucial information for material optimization and generator design, especially for waste heat recovery application where power density is more important than maximizing efficiency. The experimental system is described in detail in Sec. II along with the principles of measurements of TE parameters. One of the key improvements in the system for high temperature measurement, the thermal radiation suppression is discussed in Sec. III. The system verification with TE parameter measurements for a known sample is presented in Sec. IV.

II. EXPERIMENTAL SYSTEM

The Z-meter setup (Fig. 2) includes a high temperature heater with a measure bar and a water-chilled cold plate inside a vacuum (pressure $\sim$ 1 μTorr) system. A 1″ diameter ceramic "button" style heater (HeatWave Labs #101138) enclosed in a molybdenum radiation shield can heat the sample to a very high temperature of 1200 °C. The heater is controlled with a proportional-integral-derivative temperature controller (HeatWave Labs # 101303) to maintain the hot side temperature within an absolute accuracy of 1 °C of the set value. The measure bar stands on top of an aluminum-based cold plate connected to a water chiller (Thermo NESLAB #RTE7) outside the vacuum chamber through appropriate feed-through. A small conical shaped copper metal piece is used between the heater and a TE sample to compensate for the area difference between the two pieces; it also acts as a holder for thermocouple and electrical leads. A copper measure bar embedded with type-K thermocouples sits below the sample. The thermocouples are set in small holes drilled in the metal pieces with high temperature thermal cement to ensure good contact as well as to electrically insulate them from the metal and the sample. Two thermocouples are placed within 1 mm of the metal-thermoelectric interface to measure the hot and the cold side temperatures.

Once the TE sample is placed between the measure bar and the heater, a set of spring loaded screws are used to set and maintain high pressure ($\sim$800 psi) for good contact. In order to ensure repeatable contacts, a piezoelectric strain gauge (Omega #LCFD-100) is used to measure the pressure on the sample.

A. Principles of measurements

The measured parameters during the experiment are the open circuit voltage ($V_{oc} = V_{TE}$ at $I = 0$), the voltage across the TE sample (V_{TE}) for various input currents (I), and temperature at different points using type-K thermocouples. At each temperature setting, for each input current value, averaging the data points for voltage and thermocouple readings minimizes noise and quantization errors. A fully automated data collection system allows for a quick measurement even with long averaging.

For the thermal conductivity measurement of a single TE element, the thermal power (Q) through the measure bar is equal to the power through the sample (approximate 1-D heat flow). A finite element simulation (COMSOL) was used

TABLE I. Summary of previous Z-meter measurement for TE characterization.

Z-meter Ref.	Heater temperature (max)	Hot-side TE temperature	Temperature gradient	Thermal/electrical parasitic	Heat flux measurement technique	Electrical resistivity measurement
Classical arrangement (1965)[13]	600 °C	*600 °C (accuracy to the order to 10% achieved till 350 °C, radiation loss dominant at higher temperature)	■ $\Delta T \sim 10$ °C (thermal conductivity) ■ $\Delta T \sim 100$ °C (Seebeck coefficient)		Pyrometer used to measure heat flux through the sample	Current/voltage measurement (at zero temperature gradient)
Transient Z-meter (1990)[23]		*700 °C (results agree within 2% of the reference sample till 300 °C)			Heat flow meter used to measure thermal flux	Square wave current input, voltage measurement
Graded TE measurement setup (1998)[14]	900 °C	500 °C	$\Delta T = 385$ °C (TE couple)	Indium solder: ■ 0.5 Kcm^2/W ■ < 30 mΩ (Contact resistance variability)	Reference material (Ni) measure bar setup	Variable load resistor circuit
Effective *ZT* measurement (2009)[17]		200 °C	$\Delta T = 160$ °C		Flux sensor used to measure thermal power	Current/voltage (4-wire) ac method
Commercial Z-meter[16]		110 °C	$\Delta T = 65$–75 °C		No thermal conductivity measurement	AC resistance measurement
This work	1200 °C	440 °C	$\Delta T = 255$ °C	Dry metal contact: ■ 1.5 Kcm^2/W ■ 7 mΩ Bonded metal contact: ■ 0.05 Kcm^2/W ■ 3 mΩ (Strain gauge used to maintain reliable contact)	Au-plated Cu measure bar	Current/voltage (4-wire) active load measurement (Maximum power detection)

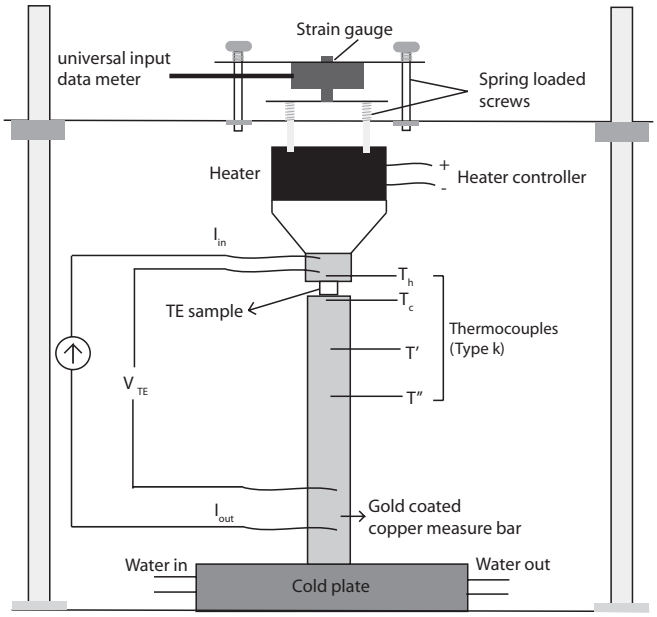

FIG. 2. Schematic of a Z-meter setup inside a vacuum chamber.

to confirm the linear temperature gradient across the measure bar for 1-D heat transfer. Two potential sources of errors in this measurement are due to convection and radiation. The high thermal conductivity of the copper helps to ensure that the temperature distribution in the measure bar rapidly approaches constant-height isotherms a short distance below the TE element, as well above where the heat transfer temperatures are taken. The experiment was performed in a vacuum environment (pressure $\sim 1\ \mu$Torr) such that air conduction and convection loss through the side walls of the apparatus and element can be neglected. The thermal conductivity for air at such low pressure (3×10^{-6} W/m.K) is nearly four orders of magnitude lower than at room pressure.[18] Due to small sample sizes and low air conductivity, the heat transfer due to side walls and air is less than 1% of the total heat flow through the sample even at high hot side temperature above 500 °C. The error due to radiation at high temperature is suppressed with low emissivity gold plated measure bar. More details on radiation suppression are discussed in Sec. II. The cross-section area of the measure bar is chosen such that the spreading resistance (units: K/W) between the sample and the metal is negligible. For the smallest sample (1.4 mm × 1.4 mm × 0.12 mm) measured using the setup, the spreading resistance is calculated according to Ref. 12, and the TE sample thermal impedance is 175 times the spreading resistance. The electrical wire contacts are held away from the thermocouples (Fig. 2) to minimize any heat conduction loss from the wires. Long length wires and thermal shielding in thermocouples are used to minimize any heat loss through them. For each measurement, two values of thermal power through the sample are obtained by combination of three thermocouple readings in the measure bar. Less than a 3% difference in the thermal power readings between the thermocouples ensure that the measurement is close to 1-D approximation. Another possible source of error in the measurement is due to the sample-metal interface in the setup, which causes a temperature difference between the thermocouple measuring the hot (T_h) (or cold (T_c)) side and the actual sample (T'_h/T'_c). The thermal resistance ($R_{\text{th,interface}}$) at the interface depends on the contact surfaces and the applied contact pressure. The heat flow through the sample and the measure bar can be depicted with a thermal equivalent circuit as shown in Fig. 3(a).

The thermal conductivity for a sample of cross-section area A_{TE}, and thickness l_{TE}, is given by

$$\kappa_{TE} = \frac{Q}{T'_h - T'_c}\left(\frac{l_{TE}}{A_{TE}}\right), \tag{2}$$

where

$$T'_h = T_h - Q \times R_{th,\text{interface}}, \tag{3}$$

$$T'_c = T_c + Q \times R_{th,\text{interface}}, \tag{4}$$

$$Q = \left(\frac{A_{bar}}{l_{bar}}\right)\kappa_{bar}(T' - T''). \tag{5}$$

Here, A_{bar} is the cross-section area of the measure bar, l_{bar} is the distance between the adjacent thermocouples in the measure bar (2 cm), and κ_{bar} is the thermal conductivity of the measure bar (copper = 391 W/m.K). T' and T'' are the temperatures recorded by type-K thermocouples in the measure bar. Q is the heat transferred through conduction.

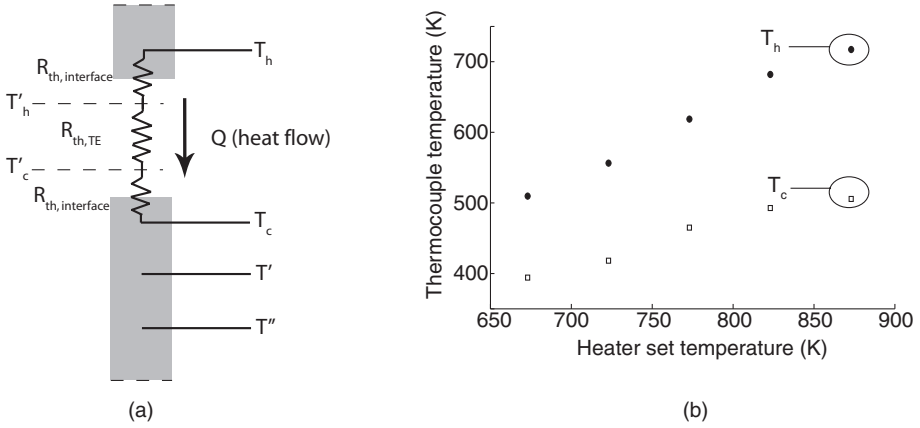

FIG. 3. (a) Thermal equivalent circuit showing interface resistances and heat flow through the sample to the measure bar; (b) thermocouple readings for the hot (T_{h}) and the cold (T_{c}) side temperature for different set heater temperatures.

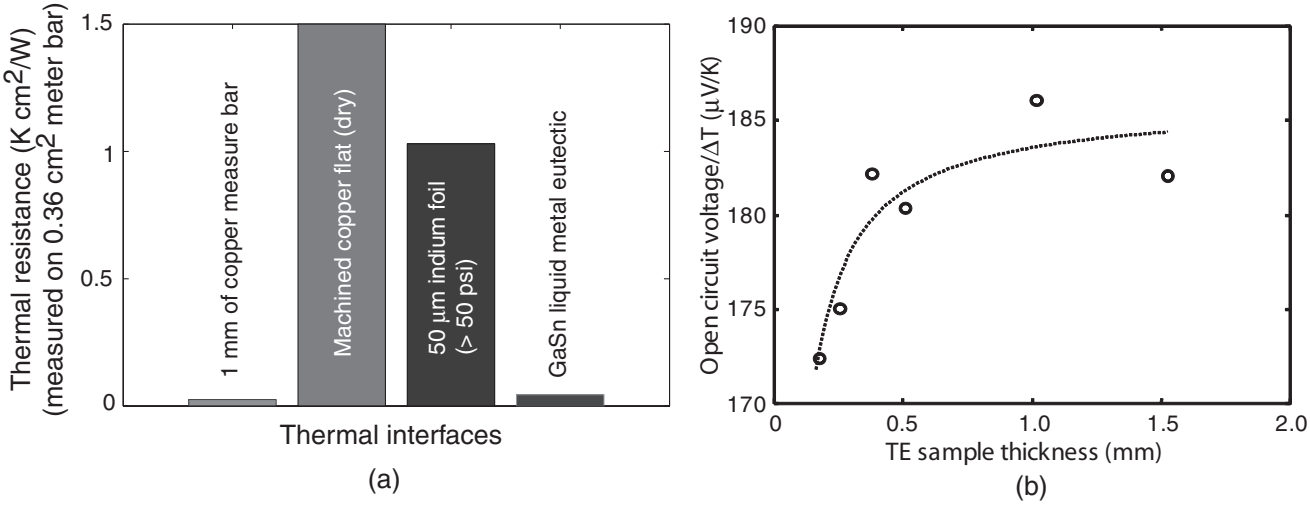

FIG. 4. (a) Contact thermal resistance for different interface material; (b) open circuit voltage over temperature gradient vs. length for Bi_2Te_3 elements (Marlow Inc.) with a best fit using the ideal "lumped Seebeck" model for the parasitic thermal contact resistance with GaSn liquid metal interfaces.

Different interface thermal resistances ($R_{\text{th,interface}}$) have been studied in Ref. 19, these are used here as a correction factor to estimate the actual temperature gradient across the sample (Fig. 4). The thermal resistance was characterized using ideal "lumped Seebeck" coefficient estimation. The variations in the ratio of the open circuit voltage over temperature gradient with length for a TE sample are due to thermal parasitics (Fig. 4(b)). A best fit can be performed to the open circuit voltage using the lumped Seebeck coefficient of the element in series with a fixed parasitic thermal resistance. For a set of measurements using a liquid metal eutectic (GaSn), the decreasing ratio of open circuit voltage over temperature gradient at short element lengths can be described by a parasitic thermal impedance of 0.05 Kcm^2/W.

The Seebeck coefficient is measured as the ratio of the open circuit voltage and the temperature gradient ($T'_h - T'_c$) across the sample

$$\alpha = \frac{V_{oc}}{T'_h - T'_c}. \tag{6}$$

A four-wire dc electrical measurement setup (Fig. 5(a)) is used to compute the resistance and the output electrical power of the sample. For a fixed temperature gradient, as the input current (I) through an external power supply is changed, the voltage (V_{TE}) across the TE sample is measured with the wire contacts. Sweeping the current across the sample and measuring the voltage provides us with the capability of having an active load equivalent across the sample. In an ideal scenario with no system parasitics, the resistance of the TE sample is equivalent to V_{TE}/I for the maximum electrical power $(IV_{\text{TE}})_{\text{max}}$ condition. The advantage of this technique is simple circuitry and very low electrical parasitic contact resistance. The four-wire measurement in Kelvin configuration eliminates the parasitic due to electric wires. Initially, an active load based on low resistance power FET circuit was used for electrical measurements (Fig. 5(b)), similar to the one described in Ref. 19. Low resistance (20 AWG) wires were used for the setup to reduce the system parasitics. The electrical parasitic resistances for both approaches are compared and the four-wire method has lower system parasitic, which is essential to measure small resistances of short-leg or thin-film TE samples. The higher parasitic in the active load setup is due to use of the current monitoring resistor and additional wires of the circuit. For the electrical measurements, the wire gauge has to be small enough to make sure the wire does not represent a parallel thermal path to the thermoelectric device under test.

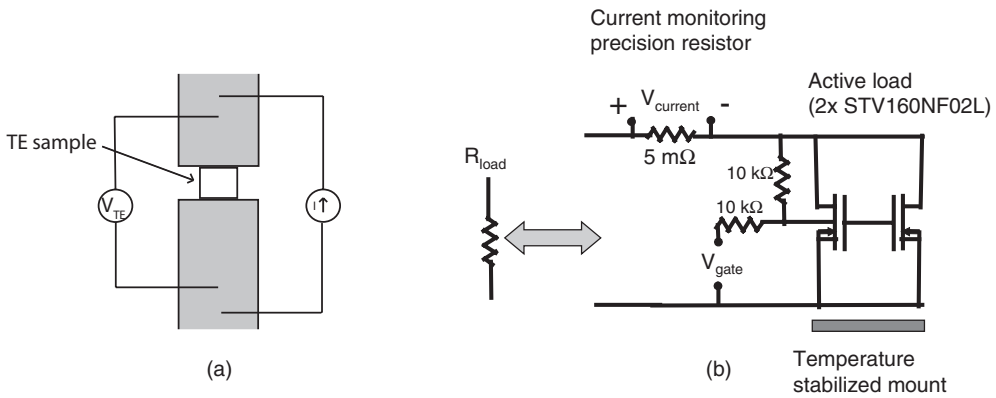

FIG. 5. (a) Active load for electrical resistivity and power measurement with current input setup; (b) active load using low resistance power FET circuitry.

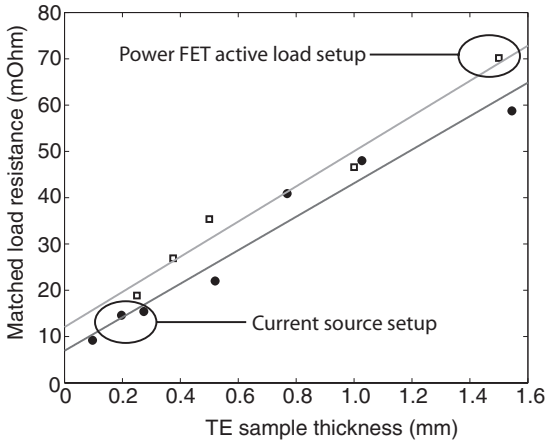

FIG. 6. Matched load resistance (□, ●) vs. thickness of MAM-Bi_2Te_3 samples (Marlow Inc.) to evaluate dry metal-metal contact parasitic, with linear fits for power FET active load system and current source setup.

Dry metal-metal interface resistance between the sample and the measure bar was measured using TE samples of a same material but different thickness. A range of Bi_2Te_3 samples from 127 μm and 508 μm was available for the study. Thicker samples were constructed by stacking 2–3 elements on top of each other. Matched load resistance for different thickness samples with a linear fit shows the setup parasitic at zero length to be 7 mΩ for the current source 4-wire setup and 12 mΩ for the power FET active load circuit (Fig. 6).

In the power generation mode, the maximum output power is measured when the load resistance is equal to the sum of the internal resistance of the TE sample and the electrical parasitics. From this matched load ($R_{\text{load}} = V_{\text{TE}}/I$ for $(IV_{\text{TE}})_{\text{max}}$), the electrical conductivity of the sample can be obtained using the following relation:

$$\sigma = \frac{1}{(R_{Load} - R_{parasitic})}\left(\frac{l_{TE}}{A_{TE}}\right). \tag{7}$$

For all the measurements performed using this setup, the electrical resistance for a single TE leg is generally small. The input current density is within the limit such that any Joule heating term is too small to have any observable effect on the overall average temperature of the sample. The temperature recorded during current sweep showed fluctuation of less than 0.5 °C for the hot and the cold side thermocouple readings.

During the same measurements, we can extract the power density (PD) and the efficiency (η), which are given by

$$PD = \frac{(IV_{TE})_{\max}}{A}, \tag{8}$$

$$\eta = \frac{(IV_{TE})_{\max}}{Q}. \tag{9}$$

For the matched load condition, where the output power is maximized, the power density increases as the thickness of the TE leg is decreased, which is why thin-film TE generators are expected to have high power density.

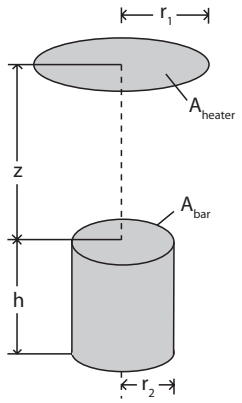

FIG. 7. Schematic for radiation error calculation from the measure bar due to the heater.

III. THERMAL RADIATION SUPPRESSION

In this experimental setup, the results rely on the fact that the thermal power through the sample is transferred to the copper measure bar via conduction (i.e., 1-D heat flow). As mentioned earlier, the convective heat loss through the sample and the measure bar is eliminated by performing the experiment in μTorr pressure range inside a vacuum chamber. As the hot side temperature is raised, the radiative heat transfer from the heater to the measure bar (a shunt path around the element) will decrease the measurement accuracy. In order to estimate the radiation error, a model for the parasitic radiative heat transfer from the heater to the measure bar is developed and experimentally validated. The radiated power is calculated from the Stefan-Boltzmann law using the geometry as shown in Figure 7 to represent the heater and the measure bar. Radiation from the side walls of the hot side is suppressed by thermal shielding. Thus only the bottom cross-section of the heater is exposed for radiation.

The total power radiated from the heater to the measure bar (q_1) is given by Equation (10), where A_{heater} is the cross-section area of the heater, $\varepsilon_{\text{heater}}$ is the emissivity, T_{heater} is the temperature of the heater, σ_{sb} is the Stefan-Boltzmann constant, and F_{12} is view factor which depends on the geometry of the heater and the bar[20]

$$q_1 = A_{heater}\varepsilon_{heater}{T_{heater}}^4\sigma_{sb}F_{12}. \tag{10}$$

Similarly, the power re-radiated by the top surface of the measure bar (q_2) is given by Equation (11), where ε_{bar} is the emissivity, and T_{bar} is the temperature of the measure bar

$$q_2 = A_{bar}\varepsilon_{bar}{T_{bar}}^4\sigma_{sb}F_{21}. \tag{11}$$

The total power transferred from the heater to the measure bar (q_3) is

$$q_3 = q_1 - q_2\varepsilon_{heater}. \tag{12}$$

And, the total power absorbed by the surface of the measure bar due to radiation from the heater (q_4) is

$$q_4 = q_3\varepsilon_{bar}. \tag{13}$$

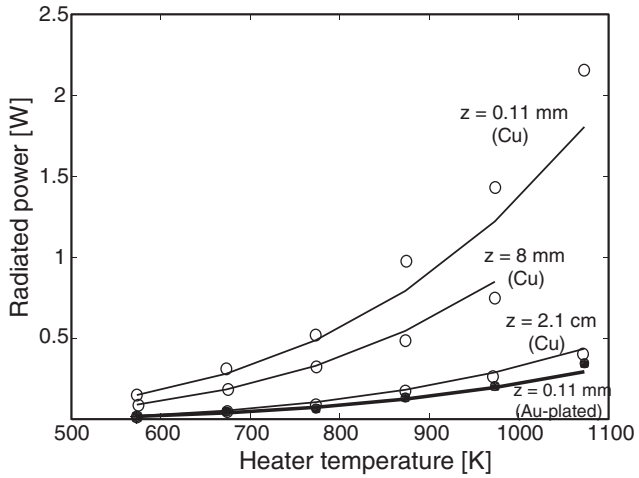

FIG. 8. Radiated power measured for copper (○) and gold-plated (●) measure bars at different heater temperatures and under different gap (z) conditions follow close to the theoretical prediction (solid lines).

For this particular geometrical setup of a cylinder and a disk, the view factor (F_{12}) is given by[21]

$$F_{12} = \frac{1}{2}\left(x - \sqrt{x^2 - 4\left(\frac{R_2}{R_1}\right)^2}\right),$$

$$\text{where } R_i = \frac{r_i}{z} \text{ and } x = 1 + \frac{1 + R_2^2}{R_1^2} \tag{14}$$

$$F_{21} = \frac{A_{heater} \times F_{12}}{A_{bar}}. \tag{15}$$

Here, r_1 and r_2 are the radii of the heater and the measure bar, respectively.

This analysis is based on the grey body assumption, where the emissivity is independent of the wavelength of the thermal radiation. In vacuum, the radiative power is measured for different heater temperature at various gaps between the measure bar and the heater. The experimental data in Figure 8 closely follow the theoretical estimation based on the above discussed relations. The parasitic radiative heat transfer is suppressed by gold coating the copper measure bar which reduces the emissivity from 0.54 for copper to 0.09 for gold. This modified apparatus suppresses radiative transfer 20-fold relative to the blackbody limit (Fig. 8). Note that coating the copper also eliminates thermal oxidation of the copper at high temperatures (>500 K), which will rapidly occur if the vacuum chamber is vented while the apparatus is still hot. This oxidation further exacerbates the radiative transfer from uncoated copper.

The radiative heat transfer with the chamber walls is estimated using the concentric cylinders geometry (chamber diameter = 18″ and measure bar diameter = $\frac{1}{4}$″). At the heater temperature of 500 °C, the estimated heat transfer between the gold-plated measure bar and the chamber walls is less than 5% of the total heat transferred via radiation to the measure bar. This heat transfer is less than 1% of the typical total heat transferred through the device under test via conduction which was small enough not to consider further.

Using such radiation suppressed measure bar setup, high temperature accurate thermal measurements of TE samples can be done, as shown in the results in Sec. IV.

IV. THERMOELECTRIC PARAMETER RESULTS

The system performance was validated by measuring bulk as well as thin-film samples which have been previously measured with conventional techniques mentioned in Sec. I. Measurements of different samples demonstrated the flexibility of the Z-meter setup going from thick samples to thin-samples, and working over wide temperature range. For a thick sample, conventional bismuth telluride (Bi_2Te_3) was measured with the Z-meter. Near room temperature (311 K), we measured a ZT of 0.87 for a 1 mm × 1 mm × 500 μm, Micro-Alloyed-Material (MAM) Bi_2Te_3 (Marlow Inc.), with a thermal parasitic correction of 1.5 Kcm^2/W (dry metal-metal contact), and a system electrical parasitic resistance of 7 mΩ. The ZT value is within 3% of the measured data provided by Marlow Inc.

For a thin-film sample, a semimetal/semiconductor nanocomposite thermoelectric material (0.6%ErAs:InGaAlAs)[22] was tested with the system. The n-type sample was approximately 1.4 mm × 1.4 mm × 60 μm. Two samples were stacked on top of each other for a total thickness of 120 μm. This relatively thin sample had gold contacts on both sides. For high temperature measurements, the heater was set at a constant temperature using the heater controller and allowed to reach steady state before taking measurements. The thermal quadrupole method[12] was used to estimate the time dependence of the thermal impedance of the setup to get to the steady state conditions. During several high temperature cross-plane measurements, it was realized that at a high applied pressure (~800 psi) metal bonding was formed between the TE sample contacts and the gold-coated metal pieces as the temperature passed certain threshold (~500 K). This bonding leads to very low thermal contact (0.05 Kcm^2/W) and system electrical parasitic (3 mΩ) compared to the dry metal-metal contacts measured earlier (Sec. II). The measurement results shown in Figures 9–13

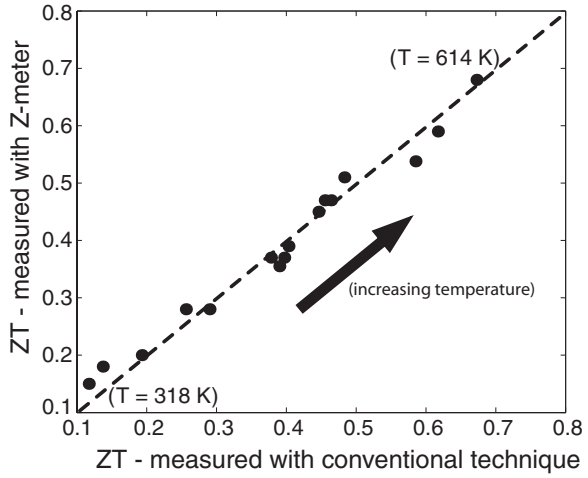

FIG. 9. ZT measurement for the n-type ErAs:InGaAlAs using the Z-meter in comparison to published result.[22]

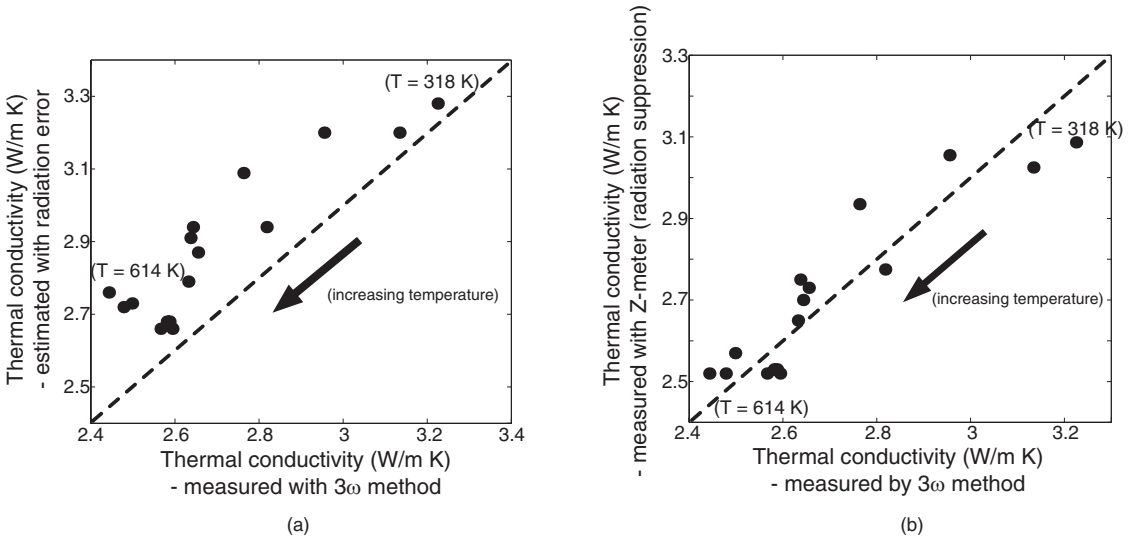

FIG. 10. (a) Thermal conductivity estimation for the TE sample in the case of no radiation suppression, compared to thermal conductivity measured with 3ω method;[22] (b) the measured thermal conductivity data vs. data from 3ω measurement.[22]

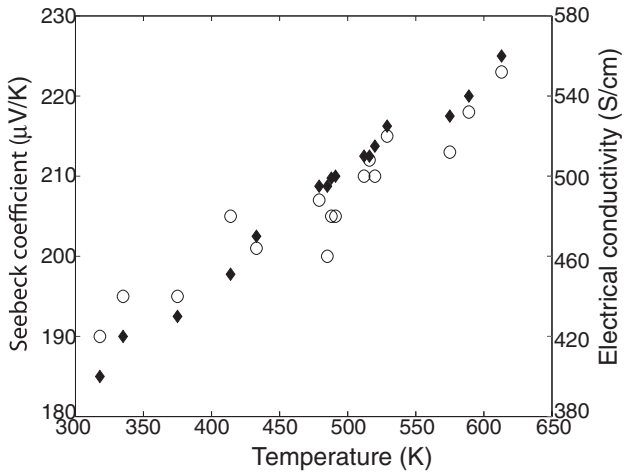

FIG. 11. Seebeck coefficient (○) and electrical conductivity (♦) measurement for the n-type ErAs: InGaAlAs sample.

represent data taken after high temperature exposure (>500 K), such that the sample was bonded to the measurement setup, and a single thermal and electrical parasitic correction factor could be used to obtain the *ZT* values.

The *ZT* data (Fig. 9) obtained from the Z-meter measurement match with less than 7% average error compared to the published data[22] for the same material. The sample was measured within an average temperature range of 300–620 K, with the highest temperature gradient of 200 K.

Looking at individual TE parameters measured with the Z-meter, the thermal conductivity for the TE sample would have had an error of 6%–7% if the measurement was done without addressing the radiation issue (Fig. 10(a)). The estimation for this erroneous thermal conductivity was done by adding the radiative power, calculated using the theory based on Sec. III, to the measured thermal power. The radiation error would have caused the measured thermal power to be higher, resulting in larger thermal conductivity than the true material value.

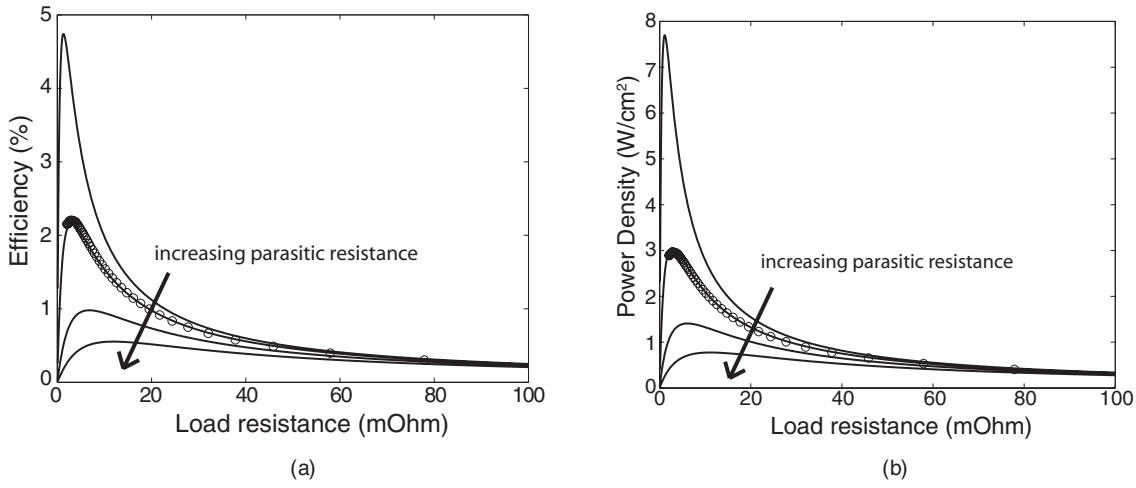

FIG. 12. (a) Efficiency and (b) power density measurement data (○) with theoretical estimations for different system parasitics at an average temperature of 614 K (best fit for $R_{parasitic} = 3$ mΩ).

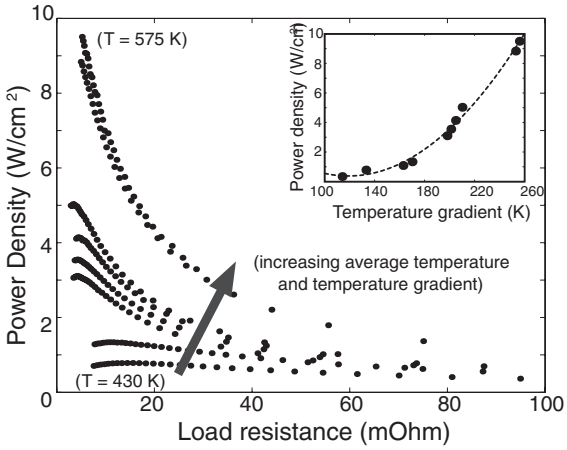

FIG. 13. Generated power density for ErAs sample at different temperature gradient and average temperature increasing from 350 K to 575 K (power density vs. temperature gradient is shown in the inset with a quadratic fit).

The measured thermal conductivity with the gold-plated measure bar shows much better results (Fig. 10(b)) with closer fit to the data from other measurement technique (3ω method).[22] Thus, without addressing the radiation issue, the Z-meter would overestimate the thermal conductivity and underestimate the overall *ZT* value with an additional 6%–7% error.

The measured temperature dependence of the Seebeck coefficient and the electrical conductivity for the sample is shown in Figure 11. The *ZT* values shown in Figure 9 are calculated by using these temperature-dependent TE parameters.

The Z-meter also gives the efficiency and the electrical power density for a single TE element. The measurement result for different load resistance at an average sample temperature of 614 K, with a temperature gradient of 200 K, is shown in Figure 12. Different load resistance across the TE sample is achieved by changing the current source. The maximum measured efficiency and the power density are limited by the system electrical parasitics. In Figure 12, the theoretical evaluation for efficiency and power density are shown with the electrical contact parasitics as the fitting parameter. The theoretical simulation with a system parasitic of 3 mΩ fits the experimental data showing very low electrical contact resistance for the setup with the bonded samples. Taking into account the system parasitics, the *ZT* value can be obtained from the efficiency measurement using the relation given by Equation (16), which relates the generator efficiency to material *ZT* in the condition of maximum power (denoted by subscript "p")[12]

$$\eta_P = \frac{T_h' - T_c'}{2T_h' - \left(\frac{T_h' - T_c'}{2}\right) + \frac{4}{Z}}. \quad (16)$$

For example, from the measured efficiency ($\eta = 2.16\%$), the *ZT* value of 0.67 was calculated which is equivalent to the value obtained from the individual TE parameters at T = 614 K.

A larger temperature gradient (>250 K) was applied across the sample to achieve high power density measurement as shown in Figure 13, but at an overall lower average sample temperature. For a single TE leg, high generated electrical power density of 9.5 W/cm^2 was measured which is 5× large than the power density for MAM-Bi_2Te_3 material[19] with the same temperature gradient.

The inset shows the power density as a function of the applied temperature difference. The data follow a parabolic profile as expected since the generated power is proportional to the square of the temperature gradient. Such thin-film TE samples with large power density at higher temperature gradient can be useful for power generation.[22]

V. CONCLUSION

In this work, we have presented an experimental technique to measure the TE parameters of a single sample at high temperature with a large temperature gradient (~200 K), similar to real-life conditions for a generator. The measurement setup was used for a wide range of temperature (300-650 K), as well as for both bulk and thin-film samples (thickness ~ 100 μm). Both thermal and electrical parasitics for the setup were carefully studied and minimized for the measurements. We developed theory for radiation loss factors and verified it experimentally at high temperature for measure bars with different emissivity. Using a gold-plated measure bar, radiation loss in the order of 6%–7% can be suppressed in the thermal measurements with the hot side temperature ranging from 330 to 718 K. TE parameters and *ZT* for a semimetal/semiconductor nanocomposite (n-type ErAs:InGaAlAs) were measured and are in good agreement with the published results measured with conventional techniques. High power density of 9.5 W/cm^2 was measured for this sample using the Z-meter under a large temperature gradient of 255 K. Such a system can provide a good platform for verification and measurement of TE parameters in conjunction with conventional techniques to assure correct measurement and reduce uncertainties by measuring all TE parameters in a single sample.

ACKNOWLEDGMENTS

The authors would like to thank Marlow Inc. for providing MAM-Bi_2Te_3 samples, and A. Shakouri (UCSC) and G. Zeng (UCSB) for ErAs:InGaAlAs samples. The work was funded by ONR MURI Thermionic Energy Conversion Center.

[1] *Handbook of Thermoelectrics*, edited by H. J. Goldsmid and D. M. Rowe (CRC, 1995), pp. 19–25.
[2] H. J. Goldsmid, *Electronic Refrigeration* (Pion, London, 1986).
[3] *Thermoelectrics Handbook - Macro to Nano*, edited by T. M. Tritt and D. M. Rowe (CRC, 2006), pp. 25–31.
[4] L. J. van der Pauw, Philips Res. Rep. **13**, 1 (1958).
[5] L. J. van der Pauw, Philips Res. Rep. **16**, 187 (1961).
[6] W. J. Parker, R. J. Jenkins, C. P. Butler, and G. L. Abbott, J. Appl. Phys. **32**, 1679 (1961).
[7] T. C. Harman, J. H. Cahn, and M. J. Logan, J. Appl. Phys. **30**, 1351 (1959).
[8] T. C. Harman, J. Appl. Phys. **30**, 1373 (1959).
[9] H. Iwasaki and H. Hori, in *Proceedings of the 24th International Conference on Thermoelectrics* (IEEE, New York, 2005), p. 513.
[10] R. Venkatasubramaniam, E. Siivola, T. Colpitts, and B. O'Quinn, Nature **413**, 597 (2001).
[11] A. E. Bowley, L. E. J. Cowles, G. J. Williams, and H. J. Goldsmid, J. Sci. Instrum. **38**, 433 (1961).

[12]P. M. Mayer, Ph.D. thesis, Massachusetts Institute of Technology, Cambridge, 2007.
[13]L. S. Phillips, J. Sci. Instrum. **42**, 209 (1965).
[14]E. Muller, J. U. Bruch, and J. Schilz, in *Proceedings for 17th International Conference on Thermoelectrics* (IEEE, New York, 1998), p. 441.
[15]K. A. T. Burkov, A. Heinrich, P. P. Konstantinov, T. Nakama, and K. Yagasaki, Meas. Sci. Technol. **12**, 264 (2001).
[16]See http://www.rmtltd.ru/tec_zmeter.htm for more information on Z-meters.
[17]A. Muto, D. Kraemer, Q. Hao, Z. F. Ren, and G. Chen, Rev. Sci. Instrum. **80**, 093901 (2009).
[18]A. Trowbridge, Phys. Rev. **2**, 58 (1913).
[19]P. Mayer and R. J. Ram, in *Proceedings of the 24th International Conference on Thermoelectrics* (IEEE, New York, 2005), p. 280.
[20]M. K. Sarivastava, V. Kumar, and S. V. G. Menon, Phys. Plasmas. **7**, 2616 (2000).
[21]K. N. Shukla and D. Ghosh, Indian J. Tech. **23**, 244 (1985).
[22]G. Zeng, J.-H. Bahk, J. E. Bowers, H. Lu, A. C. Gossard, S. L. Singer, A. Majumdar, Z. BIan, M. Zebarjadi, and A. Shakouri, Appl. Phys. Lett. **95**, 083503 (2009).
[23]*Handbook of Thermoelectrics*, edited by H. H. Woodbury, L. M. Levinson, R. S. Lewandowski, and D. M. Rowe (CRC, 1995), p. 181.